**Proceedings of the ASME 2013 International Design Engineering Technical Conferences & Computers and Information in Engineering Conference**
**IDETC/CIE 2013**
**August 4-7, 2013, Portland, USA**

**DETC2013-12895**

# NUMERICAL COMPUTATION OF NONLINEAR NORMAL MODES OF NONCONSERVATIVE SYSTEMS

**L. Renson**
Space Structures and Systems Laboratory (S3L)
Department of Aerospace and Mechanical Engineering
University of Liege
Belgium
Email: l.renson@ulg.ac.be

**G. Kerschen**
Space Structures and Systems Laboratory (S3L)
Department of Aerospace and Mechanical Engineering
University of Liege
Belgium
Email: g.kerschen@ulg.ac.be

## ABSTRACT

*Since linear modal analysis fails in the presence of nonlinear dynamical phenomena, the concept of nonlinear normal modes (NNMs) was introduced with the aim of providing a rigorous generalization of linear normal modes to nonlinear systems. Initially defined as periodic solutions, numerical techniques such as the continuation of periodic solutions were used to compute NNMs. Because these methods are limited to conservative systems, the present study targets the computation of NNMs for nonconservative systems. Their definition as invariant manifolds in phase space is considered.*

*Specifically, the partial differential equations governing the manifold geometry are considered as transport equations and an adequate finite element technique is proposed to solve them. The method is first demonstrated on a conservative nonlinear beam and the results are compared to standard continuation techniques. Then, linear damping is introduced in the system and the applicability of the method is demonstrated.*

## INTRODUCTION

NNMs are mathematical tools that offer a new framework for understanding nonlinear phenomena. They are a rigorous extension of the linear normal modes (LNMs) to nonlinear systems and were pioneered in the 1960s by Rosenberg [1, 2]. He defined an NNM as a *vibration in unison* of the system. This definition was then extended to embrace all the system's periodic solutions [3]. From this approach, several numerical techniques to compute NNMs have emerged (see, e.g., [4,5]). On the one hand, these methods are efficient and versatile methods when targeting a numerical computation of the NNMs. They pave the way for the application of the NNM theory to large-scale, complex structures [6, 7]. On the other hand, the influence of (linear and nonlinear) damping cannot be studied, which may be an important limitation in practice.

Shaw and Pierre proposed a generalization of Rosenberg's definition that provides an elegant extension of the NNM concept to damped systems. Based on geometric arguments and inspired by the center manifold theory, they defined an NNM as a two-dimensional invariant manifold in phase space [8]. A polynomial series expansion method was then introduced in order to solve the manifold partial differential equations (PDEs) and obtain the NNM geometry.

This analytical approach is usually limited to weakly nonlinear regimes and suffers from a convergence domain *a priori* unknown. The first attempt to carry out numerical computation of NNMs as invariant manifolds is that of Pesheck et al. [9, 10]. The manifold-governing PDEs are solved in modal space using a Galerkin projection with the NNM motion parametrized by amplitude and phase variables. In a recent contribution, Touzé and co-workers [11] also tackled the PDEs in modal space. They show that these PDEs can be interpreted as a transport equation, which, in turn, can be discretized using finite differences. Another interesting approach uses a Fourier-Galerkin procedure and

relies on the concept of complex nonlinear modes [12]. It does not solve the governing equations of the manifold, but it is able to compute it *a posteriori*.

The present study introduces a new method for the computation of NNMs defined as invariant manifolds in phase space. The transformation of the manifold-governing PDEs to modal space is not necessary, which means that an NNM motion is parametrized by master displacement and velocity, as in [13].

The approach developed in [10] uses global shape functions to discretize the NNM PDEs, i.e. shape functions defined over the entire computational domain. The discretization ends up with a set of highly-coupled and highly-nonlinear algebraic equations to solve. As a consequence, the computational burden was dramatically increased as the number of degree-of-freedom of the mechanical system increases and a "shift in tactics" was needed [10]. A semi-discrete approach was then introduced by dividing the amplitude domain into several sub-domains in order to reduce the complexity of the shape functions in amplitude.

Targeting the computation of NNMs for high-dimensional systems such as those encountered in industry, we propose to solve the set of PDEs using the finite element (FE) method, which employs local shape functions. The FE method renders the algorithm general and systematic. In addition, we underline the specific treatment required by the type of equations governing the NNMs. The proposed algorithm is particularly adapted to these equations.

The present paper is organized as follows. Theoretical concepts about NNMs as invariant manifold are briefly introduced. The details of the new algorithm are developed. The FE method is presented as well as our specific treatment of boundary conditions. Our algorithm is validated on a 20 DOFs system composed of a beam with a nonlinear connection. The validation procedure involves comparison with an algorithm for the continuation of periodic solution. Linear damping is introduced in the system and the applicability of the algorithm is demonstrated. Finally, a novel strategy to recover an estimation of the motion frequency is introduced and conclusions are discussed.

## NONLINEAR NORMAL MODES OF NONCONSERVATIVE SYSTEMS

A detailed description of NNMs and of their fundamental properties (e.g., frequency-energy dependence, bifurcations, and stability) is given in [3, 14] and is beyond the scope of this paper.

In the present contribution, the free response of discrete mechanical systems with $N$ degrees of freedom (DOFs) is considered, assuming that continuous systems (e.g., beams, shells, or plates) have been spatially discretized using the FE method. The equations of motion are

$$\mathbf{M}\ddot{\mathbf{x}}(t)+\mathbf{C}\dot{\mathbf{x}}(t)+\mathbf{K}\mathbf{x}(t)+\mathbf{f}_{\text{nl}}\{\mathbf{x}(t),\dot{\mathbf{x}}(t)\}=0 \qquad (1)$$

where $\mathbf{M}$, $\mathbf{C}$, and $\mathbf{K}$ are the mass, damping, and stiffness matrices, respectively; $\mathbf{x}$, $\dot{\mathbf{x}}$, and $\ddot{\mathbf{x}}$ are the displacement, velocity, and acceleration vectors, respectively; $\mathbf{f}_{\text{nl}}$ is the nonlinear restoring force vector.

To provide a rigorous definition of the NNM concept to damped systems, Shaw and Pierre defined an NNM as a two-dimensional invariant manifold in phase space [8]. Such a manifold is invariant under the flow (i.e., orbits that start out in the manifold remain in it for all time), which generalizes the invariance property of LNMs to nonlinear systems. In order to parametrize the manifold, a single pair of state variables (i.e., both the displacement and the velocity) are chosen as master coordinates, the remaining variables being functionally related to the chosen pair (Eqns. (2)).

$$\begin{aligned} x_i &= X_i(u,v), \\ y_i &= Y_i(u,v), \qquad i=1,...,N;\ i\neq k. \end{aligned} \qquad (2)$$

Using a similar approach as for the center manifold technique, the time dependence in the equations is eliminated and leads to a set of 2N-2 partial differential equations (PDEs) that can be solved for the $X_i$'s and $Y_i$'s:

$$\begin{aligned} Y_i &= \frac{\partial X_i}{\partial u}v+\frac{\partial X_i}{\partial v}f_k(u,\mathbf{X},v,\mathbf{Y}), \\ f_i(u,\mathbf{X},v,\mathbf{Y}) &= \frac{\partial Y_i}{\partial u}v+\frac{\partial Y_i}{\partial v}f_k(u,\mathbf{X},v,\mathbf{Y}), \\ & \qquad i=1,...,N;\ i\neq k, \end{aligned} \qquad (3)$$

where $\mathbf{X} = \{X_j : j=1,...,N\,;\, j\neq k\}$, $\mathbf{Y} = \{Y_j : j=1,...,N\,;\, j\neq k\}$, and $f_j$ accounts for all the forcing terms in the equations (linear/nonlinear stiffness and damping) . Equations for $i=k$ are trivially satisfied. Once the manifold-governing PDEs are solved, constraint equations (2) represent the geometrical description of the NNM. Around the equilibrium point, Eqns. (3) admit $N$ solutions, i.e., one for each mode. Geometrically, LNMs are represented by planes in phase space, and NNMs are two-dimensional surfaces that are tangent to them at the equilibrium point. The curvature of the NNM surface is purely due to nonlinear effects.

## FINITE ELEMENT COMPUTATION OF NNMs

To fit into a formulation more convenient to the FEM, Eqns. (3) are recast into Eqns. (4) where $\nabla$ is the gradient vector, and $\partial\Omega$ is the domain boundary. This boundary comprises an inflow boundary $\partial\Omega^- = \{\mathbf{u}\in\partial\Omega : \mathbf{V}(\mathbf{u}).\mathbf{n}(\mathbf{u})<0\}$ and an outflow boundary $\partial\Omega^+ = \{\mathbf{u}\in\partial\Omega : \mathbf{V}(\mathbf{u}).\mathbf{n}(\mathbf{u})>0\}$. The 2N-2 equations are quasilinear first-order hyperbolic partial differential equations that are similar to flow equations encountered in

fluid dynamics. This interpretation of the PDEs is identical to the interpretation made by Touzé and its co-workers [11] who interpreted the PDEs as a transport problem. The vector $\mathbf{V}$ can therefore be interpreted as the velocity vector of the master coordinates flow. The flow direction is called the characteristic direction and illustrates the propagation of the information into the domain.

$$\begin{cases} \mathbf{V}\cdot\nabla X_i - Y_i = 0, \\ \mathbf{V}\cdot\nabla Y_i - f_i = 0, \\ X_i|_{\partial\Omega^-} = X_i^-, \\ Y_i|_{\partial\Omega^-} = Y_i^-, \end{cases} \tag{4}$$
$$i = 1,...,N;\ i \neq k, \quad \mathbf{V}^T = \{v \ \ f_k\}$$

Figure 1(a) shows the flow of a 2 DOFs nonlinear conservative system. In the domain $\Omega$, characteristic directions form curves called characteristic curves (or characteristics). In the present case, the conservation of the energy induces closed characteristics and results in a clear distinction between the dynamics of different energies. Indeed, the "information" related to a given energy is limited to the corresponding characteristic. This illustrates there is no mixing between different energy dynamics; high and low energy dynamics do not influence each other. In the nonconservative case, characteristics spiral toward the equilibrium point of the system (here, the origin) (see Fig. 1(b)).

Solving hyperbolic PDEs requires boundary conditions at inflow ($\partial\Omega^-$), i.e. where the velocity vector $\mathbf{V}$ points inward the domain. In our first order problem, it requires to set the unknown field values ($X_i^-$, $Y_i^-$) on this boundary. However, the domain boundary is away from the equilibrium point and corresponds to a region of high-energy where no theoretical information about the manifold is available. A first (classical) strategy would be to use an extrapolation technique to estimate the unknown values at the boundary using the solution computed inside the domain. According to the above interpretation in terms of characteristics, this will involve a mixing between different energy dynamics. Extrapolation was therefore not deemed useful. Nevertheless, we note that a domain with an iso-energy curve for boundary remains everywhere tangent to the flow and boundary conditions become obsolete. Assuming two different iso-energy curves, they form the inner and outer boundaries of an annular domain. Since a clear partition of the dynamics exists, one can solve the PDEs in this region disregarding the solution computed outside it. This strategy is key to our algorithm. It avoids setting disruptive boundary conditions and reduces the computational burden. This is particularly interesting as the number of degree-of-freedom of the mechanical system becomes large.

For nonconservative systems, there is no partition of the dynamics and the flow points inward the domain boundary. However, the methodology suggested remains applicable. Indeed, let's take an annular domain whose inner and outer boundaries correspond to iso-energy curves. Generally speaking, the flow points in and out at the outer and inner boundaries; respectively. However, mathematically, an "inverse" problem where boundary conditions have to be specified at the inner boundary can be solved. The flow can be "inverted" and spiral in and out at the inner and outer boundary; respectively. A recursive strategy can then be applied to progressively solve the PDEs using the previously computed solution as boundary conditions for the next domain.

The proposed strategy suffers from a single limitation that is: iso-energy curves are only known at the solution. To circumvent this issue, a first guess of the iso-energy curve is computed using the previous domain boundary and solution. Then the shape of the new computational domain is iteratively modified as the new solution is computed. At the solution, the domain boundary fits the actual iso-energy.

### Resolution Strategy Overview

The resolution strategy is illustrated in Fig. 2. The computation starts in a small domain around the origin where the system is assumed to behave linearly. The domain boundary is established for a given initial energy and computed using a LNM. The LNM selected corresponds to the targeted NNM. The LNM is also considered as a first guess for the solution. To compute the actual solution, the domain boundary is corrected in order to fit the iso-energy corresponding to the current estimation of the solution. The correction is performed thanks to a mesh moving technique. It is applied a user-defined number of times until some criteria are fulfilled (*tolM*). Domain corrections precede each correction of the PDE solution in order to satisfy the boundary conditions. Once the solution is computed within a given accuracy *tol*, a new annular domain can be predicted. The prediction of the next iso-energy is performed using the previously computed solution. The new curve is considered as the new outer boundary whereas the old outer boundary becomes the inner one. Both boundaries define the new computational domain. The solution on this new annular region can be computed following a similar sequence of domain-correction and solution-correction. The NNM computation stops when the number of domains to compute or a maximum energy has been reached. Post-processing is performed in order to merge the different annular domains computed.

### Streamline Upwind Petrov-Galerkin

In order to solve hyperbolic PDEs using the FEM, specific numerical techniques are employed. Indeed, classical Galerkin finite element formulations using similar shape and test function spaces have demonstrated poor results, for instance, in the context of fluid dynamics [15, 16]. In a similar way to off-centered schemes in the finite difference framework, several finite element formulations deal with transport phenomena using alterna-

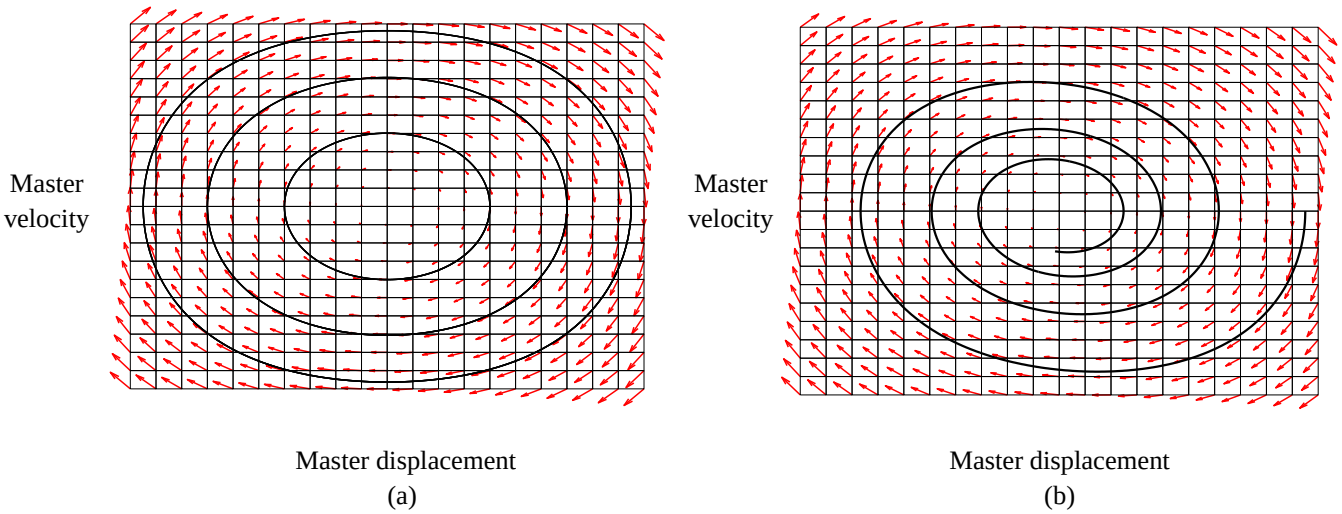


**FIGURE 1**. PDEs ARE INTERPRETED AS FLOW EQUATIONS WHERE **V** DESCRIBES THE VELOCITY FIELD (→). (a) FOR A CONSERVATIVE SYSTEM, THE FLOW IS TANGENT TO ISO-ENERGY CURVES. (b) FOR A NONCONSERVATIVE SYSTEM, THE FLOW SPIRALS TO THE EQUILIBRIUM POINT.

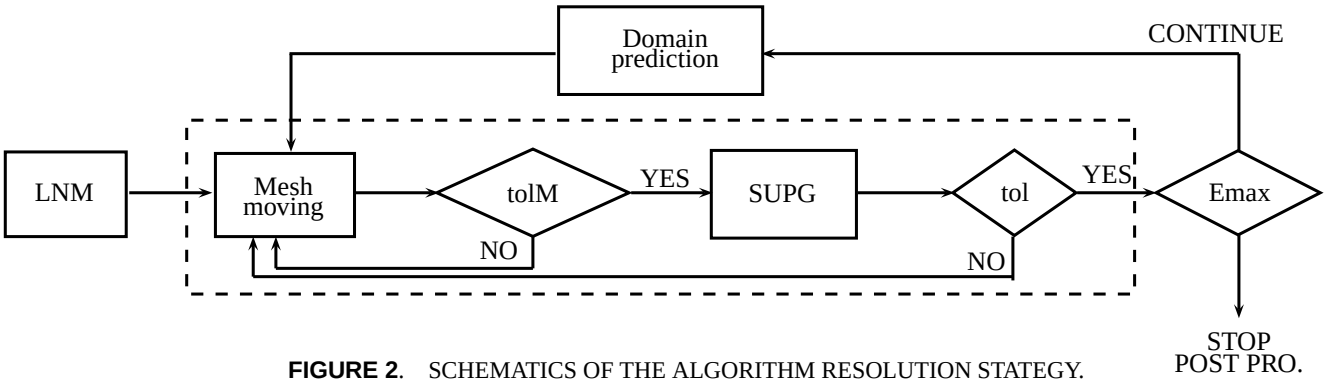


**FIGURE 2**. SCHEMATICS OF THE ALGORITHM RESOLUTION STATEGY.

tive test functions. The SUPG method is used herein and consists in over-weighting the shape functions that are upstream. This method falls within the general category of Petrov-Galerkin formulations where test and shape functions are taken in different spaces. The approach is rather standard and its description is out of the scope of our paper. We briefly present the major points of our formulation and the interested reader can refer to [15] for practical details about SUPG.

To derive our finite element formulation, a weighted residual approach is applied to Eqns. (4). The formulation is presented in Eqns. (5) where $i = 1,\ldots,N$ with $i \neq k$ and where shape functions are considered as simple first-order Lagrange shape functions: $N^b \in \mathbb{P}^1$. The test functions are $\tilde{N}^b = N^b + \tau \mathbf{V}.\nabla N^b$. As already mentioned, test functions differ from classical Galerkin test functions via an upstream overweighting ($\tau \mathbf{V}.\nabla N^b$). As a consequence, discontinuous test functions are employed [17].

$$\int\int_\Omega [\mathbf{V}(u,v,\mathbf{X},\mathbf{Y}) \cdot \nabla X_i(u,v) - Y_i(u,v)]\, \delta\tilde{Y}_i \, dudv = 0$$
$$\int\int_\Omega [\mathbf{V}(u,v,\mathbf{X},\mathbf{Y}) \cdot \nabla Y_i(u,v) - f_i(u,v,\mathbf{X},\mathbf{Y})]\, \delta\tilde{X}_i \, dudv = 0 \quad (5)$$

The parameter $\tau$ can be defined according to various definitions [18–21]. Here, $\tau = \frac{h^e}{2||V||_2}$.

After the FE discretization, the set of PDEs is transformed to a set of coupled nonlinear algebraic equations. These equations are solved using a Newton-Raphson procedure where the Jacobian matrix is provided analytically. Each iteration involves the solution of a large linear system. It is computed using the GMRes ("Generalized Minimal Residual") iterative solver and left and right ILU preconditioners ("Incomplete LU"). An important feature of our problem is that equations to solve remains nonlinear even if the mechanical system considered is linear.

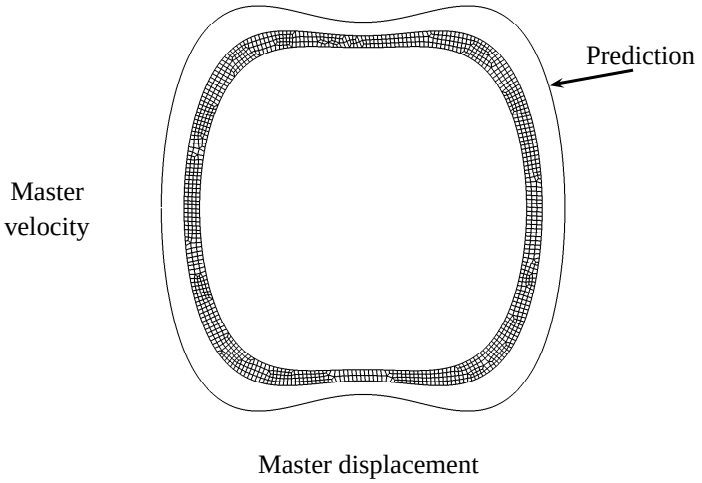


**FIGURE 3**. PREDICTION OF THE NEXT DOMAIN BOUNDARY USING THE LAST CONVERGED SOLUTION.

### Domain Prediction

The prediction of the domain $d+1$ is performed using an approach similar to continuation. Consider the outer boundary $E^d$. This outer boundary becomes the inner boundary of the next domain $d+1$. To compute the new outer boundary, an energy increment $\Delta E^d$ is applied and an estimation of the iso-energy curve at $E^{d+1} = E^d + \Delta E^d$ is determined. Linearizing the energy around each point $i$ of the boundary $d$ and solving Eqn. (6) transforms energy increments in terms of displacements $(\Delta u_i, \Delta v_i)$ to apply to boundary nodes. Figure 3 illustrates the result of this procedure.

$$\Delta E^d = \frac{dE}{du}|^{d,i} \Delta u_i + \frac{dE}{dv}|^{d,i} \Delta v_i, \quad \forall i. \tag{6}$$

### Domain Correction using a Mesh Moving Technique

As introduced, the shape of the computational domain is chosen in order to avoid imposing boundary conditions. Such a domain needs to be everywhere tangent to the flow $\mathbf{V}$. In the particular case of a conservative system, the flow is everywhere tangent to iso-energy curves. An iso-energetic domain boundary would therefore meet our requirement. Unfortunately, such curves are known at the solution and only a prediction of it can be performed. In order to satisfy the need of boundary conditions to solve the hyperbolic problem, the domain is modified at each iteration such that it is an iso-energy curve for the current estimation of the solution. At each iteration, BCs are thus satisfied and the hyperbolic problem is well posed.

To modify the domain's shape, the mesh is considered as a pseudo-elastic medium and a linear elasticity problem is solved. The inner boundary is considered as clamped (displacements are set to zero) while the outer boundary is moved in order to equal a reference energy. This reference energy is considered to be the smallest energy of all boundary points. This choice has the advantage to consider a new boundary completely enclosed into the previous one. The data interpolation between both meshes is therefore obvious and does not require any extrapolation. The formula used to compute the displacements imposed to the boundary nodes are similar to formula used for domain prediction (cf. Eqn. (6)). The only difference is the energy increment $\Delta E$ that is now determined to equal the reference energy.

Without going into the details of mesh moving techniques, the finite element method discretization results in a linear algebraic problem (Eqn. (7)) where $\mathbf{K}^{\text{el.}}$ denotes the stiffness matrix of the discretized domain considered as a pseudo-elastic medium. The displacements $\mathbf{q}$ are split into three different sets, namely: clamped nodes whose displacements equal zero ($\mathbf{q}_0 = \mathbf{0}$), outer nodes whose displacements are non-zero and follow the energy corrections ($\mathbf{q}_d$), and finally internal nodes whose displacements are unknown ($\mathbf{q}_i$). This partition provides a straightforward expression for the unknown displacements $\mathbf{q}_i$ (Eqn. (7)). Additional information about mesh moving techniques can be found in [22].

$$\begin{bmatrix} \mathbf{K}_{ii} & \mathbf{K}_{id} & \mathbf{K}_{i0} \\ \mathbf{K}_{di} & \mathbf{K}_{dd} & \mathbf{K}_{d0} \\ \mathbf{K}_{0i} & \mathbf{K}_{0d} & \mathbf{K}_{00} \end{bmatrix}^{\text{el.}} \begin{bmatrix} \mathbf{q}_i \\ \mathbf{q}_d \\ \mathbf{q}_0 \end{bmatrix} = \mathbf{0} \Rightarrow \mathbf{q}_i = -\mathbf{K}_{ii}^{-1} \mathbf{K}_{id} \mathbf{q}_d \tag{7}$$

Mesh modification according to iso-energy curves is critical and can lead to erroneous results or even divergence if not performed. Indeed, the correction should be applied enough times in order to have a domain which is consistent with the current estimation of the solution. Without proper boundary conditions, the problem to solve is not well posed and the PDE resolution will fail.

### Convergence Study

In this section, we investigate the convergence rate of our method on the out-of-phase mode of a 2DOF system including a cubic nonlinearity. Calculations are performed using a reference periodic solution as exact domain boundary in order to artificially satisfy the boundary conditions and to free the results from the mesh-moving influence. The convergence rate for triangular and quadrangular first order elements is presented in Fig. 4. The convergence rate for triangles is 1.70 and for quadrangles is 1.94. In a linear setting, the convergence rate of the SUPG method was demonstrated [23] to be suboptimal with a convergence rate of $O(h^{3/2})$ (i.e. a *gap* of $h^{1/2}$ with the optimal rate of $O(h^2)$). In practice, the $L^2$ convergence rate appeared to vary between $O(h^{3/2})$ and $O(h^2)$ depending on mesh parameters [24]. In the present situation, we observe an almost optimal convergence

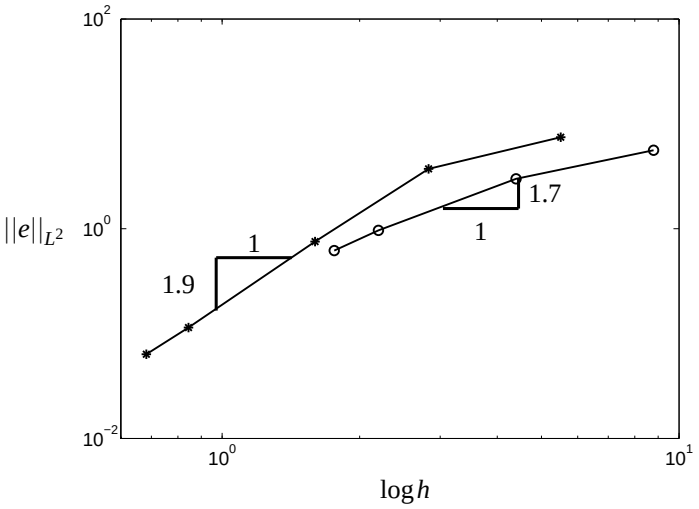


**FIGURE 4**. $L^2$-NORM CONVERGENCE FOR TRIANGLES AND QUADRANGLES. (-*-) FOR QUADRANGLES AND (-o-) FOR TRIANGLES.

rate for quadrangular elements and an improved convergence rate with respect to theoretical expectations for triangles.

## A NONLINEAR CONSERVATIVE BEAM

In this section, the algorithm developed is demonstrated on a linear conservative beam (see Fig. 5) beam with nonlinear boundary conditions. The beam is discretized using 10 beam elements resulting in a system with 20 DOFs (i.e. 38 unknown fields have to be solved). A cubic spring is attached to the end of the beam and models a geometrical nonlinearity induced by the large displacements of a thin element at the end of the beam.

For conservative systems, reference algorithms to compute NNMs exist [4, 5]. For instance, the "exact" manifolds can be computed using the technique developed in [5], which combines shooting and pseudo-arclength continuation. For each NNM, the graphical depiction in phase space of the periodic orbits at different energy levels provides a reference solution to which we can compare the solution computed using the invariant manifold approach. Figure 6 presents the first NNM of the system for the slave angular velocity of the ninth beam-element ($Y_{19}$). The results coming from the invariant manifold approach are depicted in green whereas the reference solutions are in yellow. A very good agreement between computed and reference surfaces is observed (green and yellow are "intimately mixed").

A more quantitative comparison of the results is now carried out. The initial conditions in the modal space $(u,v)$ of the first (bending) mode computed through the FE method are transformed back to physical space $(x_1,y_1,x_2,y_2)$ using Eqn. (2). Both the equations of motion in physical space (1) and in modal space (8) are numerically integrated for these initial conditions using

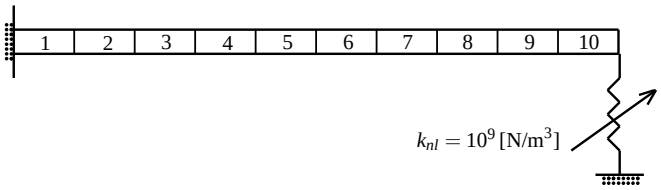


**FIGURE 5**. NONLINEAR BEAM SYSTEM. THE BEAM PARAMETERS ARE: $E = 2.05e11$ $[Pa]$, $\rho = 7800$ $[Kg/m^3]$, LENGTH $= 0.7$ $[m]$, WIDTH $= 0.014$ $[m]$, HEIGHT $= 0.014$ $[m]$, $I_x = 0.014^4/12$ $[m^4]$. THE FULL BEAM IS DISCRETIZED USING 10 BEAM ELEMENTS (20 DOFs).

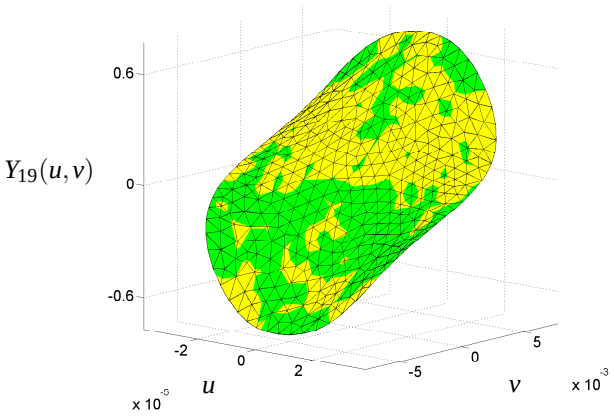


**FIGURE 6**. SLAVE VELOCITY $Y_{19}$ MANIFOLD IN FUNCTION OF THE MASTER COORDINATES $(u,v)$ FOR THE FIRST NNM. THE RESULTS FROM THE INVARIANT MANIFOLD APPROACH (GREEN) ARE IN EXCELLENT AGREEMENT WITH THE REFERENCE (YELLOW).

Runge-Kutta method.

$$\begin{aligned} \dot{u} &= v, \\ \dot{v} &= f_k(u,\mathbf{X}(u,v),v,\mathbf{Y}(u,v)), \qquad i = 1,...,N;\ i \neq k. \end{aligned} \tag{8}$$

The resulting time series in modal space are then transformed back to physical space and compared to the time series generated directly in physical space. The quantitative comparison is achieved using the normalized mean-square error (NMSE):

$$\mathrm{NMSE}(\hat{f}) = \frac{100}{N\sigma_f^2}\sum_{i=1}^{N}(f(i)-\hat{f}(i))^2 \tag{9}$$

where $\hat{f}$ is the time series to be compared to the reference series $f$, $N$ is the number of samples and $\sigma_f^2$ is the variance of

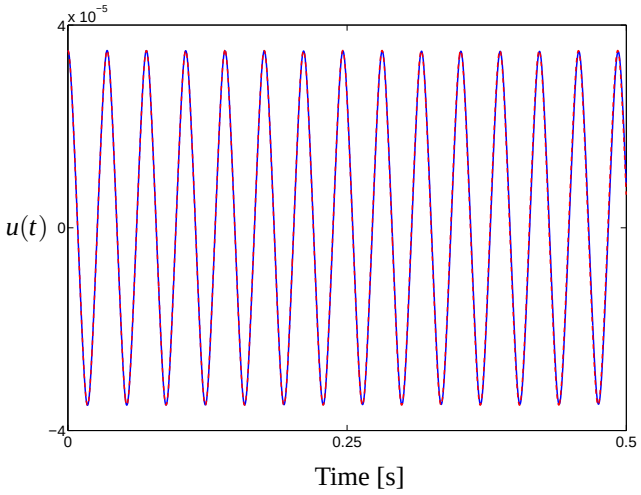


**FIGURE 7**. MASTER DISPLACEMENT DYNAMICS FOR THE REDUCED (BLUE) AND FULL-SYSTEM (RED). A VERY GOOD AGREEMENT IS OBSERVED.

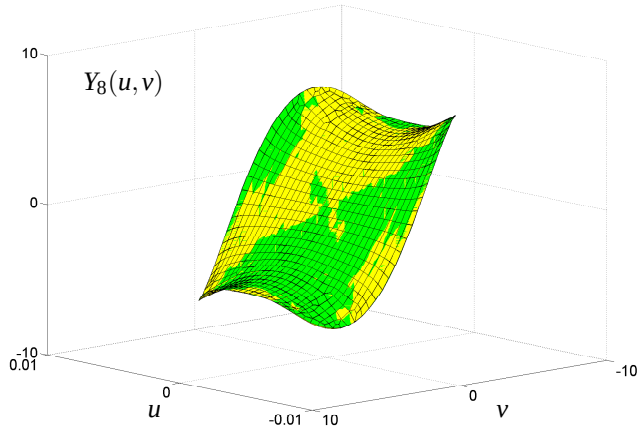


**FIGURE 8**. SLAVE VELOCITY $Y_8$ MANIFOLD IN FUNCTION OF THE MASTER COORDINATES $(u,v)$ FOR THE SECOND NNM. THE RESULTS FROM THE INVARIANT MANIFOLD APPROACH (GREEN) ARE IN EXCELLENT AGREEMENT WITH THE REFERENCE (YELLOW).

the reference time series. A NMSE value of 1% is commonly assumed to reflect excellent concordance between the time series. Figure 7 compares the dynamics reduced on the invariant manifold and the full-system dynamics. A excellent agreement between the different time series is observed over more than 15 periods. It especially indicates a very accurate capture of the motion frequency (in addition to the motion amplitude capture). The NMSE of 0.1% confirms our observations.

Figure 8 presents the second NNM for the velocity field of a DOF located close the middle of beam. Contrary to the first mode where the bending of the surface appears for DOFs close to the beam tip, larger surface deformations are observed for DOFs in the middle of the beam. This observation is consistent with the modal shape of both linear modes. In both cases, the NNMs surface deformation is more evidenced for velocity coordinates than displacement ones. For this second NNM, a quantitative comparison with the NMSE reveals a perfect matching between reduced and full-system time series. The NMSE is 1e-4% over more than 20 periods.

## A NONLINEAR NONCONSERVATIVE BEAM

In this section, the same beam-example is considered. Linear proportional damping is however introduced in the system. The damping matrix satisfies: $\mathbf{C} = \alpha\mathbf{M} + \beta\mathbf{K}$ where $\alpha = 5$ and $\beta = 5e-6$. The linear modal damping coefficient for the first mode is 0.7%.

Figure 9 presents the solution obtained for the damped system and compares it to the conservative results. One can observe that due to the proportionality of the damping, both surfaces coincide around the origin. This observation can be extended to

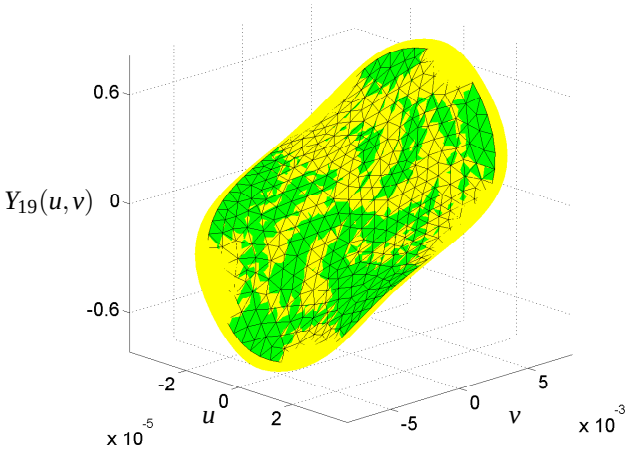


**FIGURE 9**. SLAVE VELOCITY $Y_{19}$ MANIFOLD IN FUNCTION OF THE MASTER COORDINATES $(u,v)$ FOR THE FIRST NNM. THE MANIFOLD FOR THE CONSERVATIVE SYSTEM (GREEN) AND THE NONCONSERVATIVE SYSTEM (YELLOW) HAVE THE SAME SHAPE.

larger amplitudes where the manifold bends. It is explained by the proportional nature of the damping that does not affect the linear modal shapes.

In the presence of damping, no reference results are available and results validation relies only on time integration. Figure 10 compares the dynamics reduced (blue) on the invariant

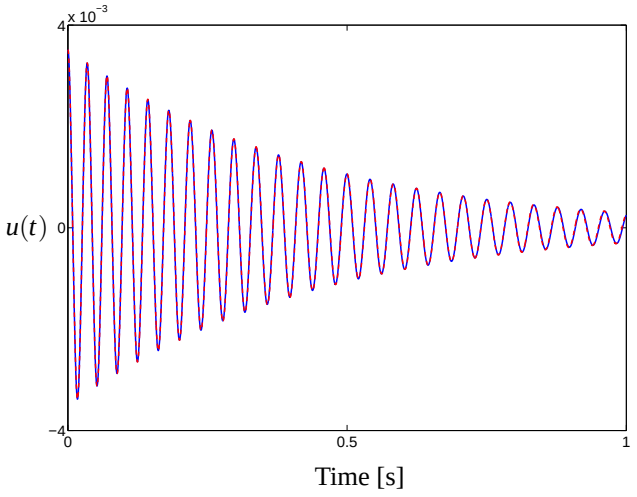


**FIGURE 10**. MASTER DISPLACEMENT DYNAMICS FOR THE REDUCED (BLUE) AND FULL-SYSTEM (RED). A VERY GOOD AGREEMENT IS OBSERVED.

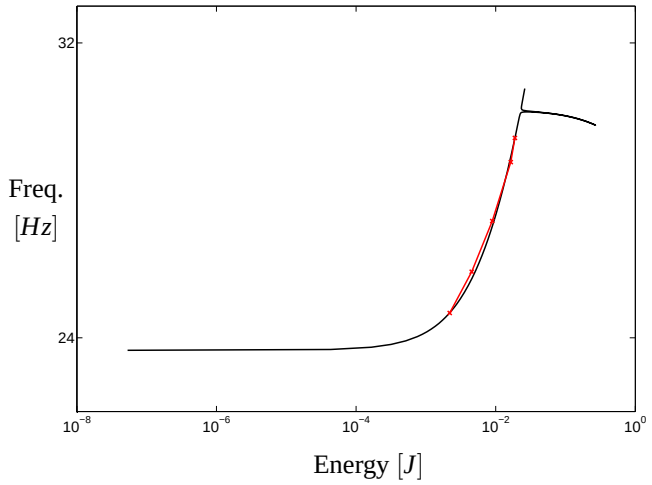


**FIGURE 11**. FREQUENCY COMPUTED USING THE INVARIANT MANIFOLD APPROACH (-*-) IS IN GOOD AGREEMENT WITH THE REFERENCE (–). REFERENCE RESULTS COMPUTED USING NEWMARK ALGORITHM AND $10^3$ POINTS PER PERIOD.

manifold and the full-system dynamics (red). The NMSE value of 0.06% confirms the perfect matching observed and the accuracy of the FE solution.

## FREQUENCY COMPUTATION

A key step in the derivation of the PDEs governing the manifold is the removal of the time dependence of the equations. As a consequence, time does not appear anymore in the equations and NNMs are geometrically described with PDEs. Therefore, contrary to methods using the system's ODEs where an explicit time dependence is present, the invariant manifold approach does not provide a straightforward access to the motion frequency.

However, in the restrictive case of conservative systems, "post-processing" operations can be applied in order to combine standard continuation techniques on the reduced-dynamic ODEs (see Eqns. (8)). In the present study, we developed a novel approach to estimate the motion frequency as a byproduct of our finite element strategy. This approach is based on the interpretation of PDEs as hyperbolic equations and on the "iso-energetic" resolution strategy we employ. It does not rely on the reduced-dynamic ODEs, so time integration and and continuation are not needed.

PDEs are solved in the $\Omega$ $(u,v)$ plane where each domain boundary corresponds to an iso-energy curve. If the reduced dynamics was integrated on one of these curves, all the points belonging to the time series would geometrically lie on a domain boundary. Therefore the points describing the contour of the finite element mesh also belong to this time series and the contour corresponds to one period of motion. In order to compute the motion frequency, the contour length is divided by the averaged norm of the velocity $\mathbf{V}$ along each edge. Figure 11 compares the first NNM frequency computed using the above approach (red) with classical continuation techniques (black). We observe a very good agreement between both frequency-energy plots. Note that the discretization of the red curve corresponds to the energy step-size performed by the FE algorithm during the NNM computation. This method has not been yet extended to nonconservative systems. The main reason is that the flow is not anymore tangent to the domain boundary.

## CONCLUSIONS

Despite NNMs have proven versatile and helpful in understanding the dynamics of nonlinear systems, the study of the influence of damping in NNMs is key to their development in an industrial framework. In this paper, we developed a novel algorithm for the computation of NNMs of nonconservative systems. Thanks to the FE method, the algorithm is geared toward large-scale systems.

Specifically, this paper first highlighted the hyperbolic nature of the PDEs (transport phenomenon) and, based on this observation, we proposed specific numerical treatments. The FE formulation (SUPG) is properly suited to our equations and the resolution strategy accounts for the boundary conditions using annular-ring domains with iso-energy boundaries. A mesh moving technique is employed to correct the shape of the domain. The algorithm was first demonstrated on a MDOF conservative system. The computation of the NNM and the resulting dynamics were both very accurate. Then we demonstrated that the developed algorithm was also applicable to nonconservative sys-

tems.


## ACKNOWLEDGMENT

The author L. Renson would like to acknowledge the Belgian National Fund for Scientific Research (FRIA fellowship) for its financial support.


## REFERENCES


[1] Rosenberg, R. M., 1966. "On nonlinear vibrations of systems with many degrees of freedom". *Advances in Applied Mechanics,* ***Volume 9***, pp. 155–242.

[2] Rosenberg, R. M., 1962. "The normal modes of nonlinear n-degree-of-freedom systems". *Journal of Applied Mechanics*, p. 8.

[3] Kerschen, G., Peeters, M., Golinval, J. C., and Vakakis, A. F., 2009. "Nonlinear normal modes, part I: A useful framework for the structural dynamicist". *Mechanical Systems and Signal Processing,* ***23***(1), pp. 170–194.

[4] Arquier, R., Bellizzi, S., Bouc, R., and Cochelin, B., 2006. "Two methods for the computation of nonlinear modes of vibrating systems at large amplitudes". *Computers & Structures,* ***84***(24-25), pp. 1565–1576.

[5] Peeters, M., Viguié, R., Srandour, G., Kerschen, G., and Golinval, J. C., 2009. "Nonlinear normal modes, part II: Toward a practical computation using numerical continuation techniques". *Mechanical Systems and Signal Processing,* ***23***(1), pp. 195–216.

[6] Peeters, M., Kerschen, G., Golinval, J. C., and Stephan, C., 2011. "Nonlinear normal modes of real-world structures: Application to a full-scale aircraft". *ASME Conference Proceedings,* ***2011***(54785), pp. 475–492.

[7] Renson, L., Noël, J., Kerschen, G., and Newerla, A., 2012. "Nonlinear modal analysis of the SmallSat spacecraft". In the Proceedings of the European Conference on Spacecraft Structures, Materials and Environmental Testing.

[8] Shaw, S. W., and Pierre, C., 1991. "Non-linear normal modes and invariant manifolds". *Journal of Sound and Vibration*, p. 4.

[9] Pesheck, E., 2000. "Reduced order modeling of nonlinear structural systems using nonlinear normal modes and invariant manifolds". PhD thesis.

[10] Pesheck, E., Pierre, C., and Shaw, S. W., 2002. "A new Galerkin-based approach for accurate non-linear normal modes through invariant manifolds". *Journal of Sound and Vibration,* ***249***(5), pp. 971–993.

[11] Blanc, F., Touzé, C., Mercier, J. F., Ege, K., and Bonnet Ben-Dhia, A. S. "On the numerical computation of nonlinear normal modes for reduced-order modelling of conservative vibratory systems". *Mechanical Systems and Signal Processing*.

[12] Laxalde, D., and Thouverez, F., 2009. "Complex non-linear modal analysis for mechanical systems: Application to turbomachinery bladings with friction interfaces". *Journal of Sound and Vibration,* ***322***(45), pp. 1009–1025.

[13] Shaw, S. W., and Pierre, C., 1993. "Normal modes for non-linear vibratory systems". *Journal of Sound and Vibration,* ***164***, p. 40.

[14] A.F. Vakakis, L.I. Manevitch, Y. M. V. P. A. Z., 1996. *Normal Modes and Localization in Nonlinear Systems*. John Wiley & Sons, New York.

[15] Donea, J., and Huerta, A., 2005. *Steady Transport Problems*. Finite Element Methods for Flow Problems. John Wiley & Sons, Ltd.

[16] Brooks, A. N., and Hughes, T. J. R., 1982. "Streamline upwind/Petrov-Galerkin formulations for convection dominated flows with particular emphasis on the incompressible Navier-Stokes equations". *Computer Methods in Applied Mechanics and Engineering,* ***32***(1-3), pp. 199–259.

[17] Hughes, T. J. R., and Tezduyar, T. E., 1984. "Finite element methods for first-order hyperbolic systems with particular emphasis on the compressible Euler equations". *Computer Methods in Applied Mechanics and Engineering*, p. 68.

[18] Knobloch, P., 2008. "On the definition of the SUPG parameter.". *Electronic Transactions on Numerical Analysis,* ***32***, pp. 76–89.

[19] Tezduyar, T. E., and Osawa, Y., 2000. "Finite element stabilization parameters computed from element matrices and vectors". *Computer Methods in Applied Mechanics and Engineering,* ***190***(3-4), pp. 411–430.

[20] Akin, J. E., and Tezduyar, T. E., 2004. "Calculation of the advective limit of the SUPG stabilization parameter for linear and higher-order elements". *Computer Methods in Applied Mechanics and Engineering,* ***193***(21-22), pp. 1909–1922.

[21] Codina, R., Onate, E., and Cervera, M., 1992. "The intrinsic time for the streamline upwind/Petrov-Galerkin formulation using quadratic elements". *Computer Methods in Applied Mechanics and Engineering,* ***94***(2), pp. 239–262.

[22] Stein, K., Tezduyar, T. E., and Benney, R., 2004. "Automatic mesh update with the solid-extension mesh moving technique". *Computer Methods in Applied Mechanics and Engineering,* ***193***(21-22), pp. 2019–2032.

[23] Johnson, C., Nvert, U., and Pitkranta, J., 1984. "Finite element methods for linear hyperbolic problems". *Computer Methods in Applied Mechanics and Engineering,* ***45***(13), pp. 285–312.

[24] Zhou, G., 1997. "How accurate is the streamline diffusion finite element method?". *Mathematics of Computation,* ***66***(217), pp. 31–44.